

Resistivity in the Vicinity of a van Hove Singularity: Sr_2RuO_4 under Uniaxial Pressure

M. E. Barber,^{1,2,*} A. S. Gibbs,^{1,†} Y. Maeno,³ A. P. Mackenzie,^{1,2,‡} and C. W. Hicks^{2,§}

¹Scottish Universities Physics Alliance, School of Physics and Astronomy,
University of St. Andrews, St. Andrews KY16 9SS, United Kingdom

²Max Planck Institute for Chemical Physics of Solids, Nöthnitzer Straße 40, 01187 Dresden, Germany

³Department of Physics, Graduate School of Science, Kyoto University, Kyoto 606-8502, Japan

 (Received 6 September 2017; published 14 February 2018)

We report the results of a combined study of the normal-state resistivity and superconducting transition temperature T_c of the unconventional superconductor Sr_2RuO_4 under uniaxial pressure. There is strong evidence that, as well as driving T_c through a maximum at ~ 3.5 K, compressive strains ϵ of nearly 1% along the crystallographic [100] axis drive the γ Fermi surface sheet through a van Hove singularity, changing the temperature dependence of the resistivity from T^2 above, and below the transition region to $T^{1.5}$ within it. This occurs in extremely pure single-crystals in which the impurity contribution to the resistivity is < 100 n Ω cm, so our study also highlights the potential of uniaxial pressure as a more general probe of this class of physics in clean systems.

DOI: 10.1103/PhysRevLett.120.076602

When the shape or filling of a Fermi surface is changed such that the way it connects in momentum (k) space changes, or it disappears altogether, its host metal is said to have undergone a Lifshitz transition [1]. This zero-temperature transition has no associated local Landau order parameter and is one of the first identified examples in condensed matter physics of a topological transition. Lifshitz transitions are associated with anomalies in the density of states known as van Hove singularities (VHS), arising due to the appearance of points or, in the presence of interactions, regions in k space where the local density of states diverges [2]. In materials with two-dimensional electronic structures, the integrated density of states also diverges. Lifshitz transitions are therefore associated with formation or strengthening of ordered states, with superconductivity [3–6] and magnetism [7,8] among the most prominently studied examples. They are also expected, even in the absence of order, to affect the electrical transport [4,9,10].

It is therefore of considerable interest to tune materials through Lifshitz transitions. However, it is challenging to do so cleanly. Nonstoichiometric doping can be employed to continuously tune the filling of a band, however, doing so introduces disorder, which always complicates understanding of the observed response. Lifshitz transitions can be driven by magnetic field, coupling through the Zeeman term [11–16]. However, the range of materials in which the bandwidth is sufficiently narrow for laboratory-accessible magnetic fields to reach a Lifshitz transition is limited, and the field itself can also couple constructively or destructively to many forms of order.

Hydrostatic pressure can drive Lifshitz transitions [17], when it is strong enough to change the relative band filling

in multiband materials or to substantially change the shape of a Fermi surface. As illustrated in Fig. 1, equal uniaxial pressure can, in general, drive much larger changes in Fermi surface shape. Lifshitz transitions have been achieved in the three-dimensional superconducting metals aluminium [18] and cadmium [22] through uniaxial tensioning of single-crystal whiskers. The effect was observable but not large, with the superconducting transition temperature T_c , for example, changing by only ~ 20 mK. Generically, a much stronger effect is expected in materials with quasi-2D electronic structures.

We have recently developed novel methods to apply high uniaxial pressure to larger samples [23,24]. In this Letter, we report simultaneous electrical resistivity and magnetic susceptibility measurements on the multiband metal Sr_2RuO_4 under uniaxial compressive strains of up to 1%. The superconductivity of Sr_2RuO_4 is very well studied

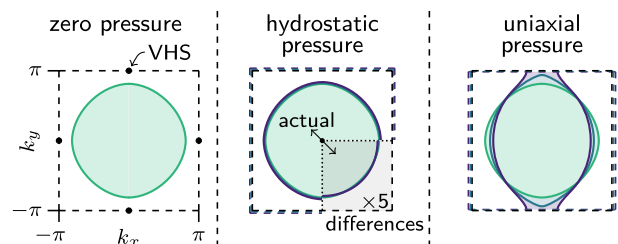


FIG. 1. An illustrative single-band tight-binding model depicting the changes of a two-dimensional Fermi surface under hydrostatic versus uniaxial pressure. In general, hydrostatic pressure increases the relative weight of next-neighbor hopping terms, causing large Fermi surfaces to become more circular [19]. An equal uniaxial pressure can drive much larger distortions. Simulation parameters are given in [20].

[25–29]. In first-principles calculations, Sr_2RuO_4 is predicted to undergo a Lifshitz transition when the lattice is compressed by $\sim 0.75\%$ along a $\langle 100 \rangle$ lattice direction [30]. A tight-binding model of this transition is shown in Fig. 2(a): the topology of the γ Fermi surface sheets changes, while the other two sheets are much less strongly affected. In previous work, we have shown that T_c passes through a pronounced peak at a uniaxial compressive strain of $\sim 0.6\%$. It is tempting to associate this peak with the Lifshitz transition; however, there are other possibilities. For example, the peak could mark the onset of strain-induced magnetic order [32]. Therefore, for more evidence, here we closely investigate the electrical resistivity of the normal state over this strain range.

A schematic of our experimental apparatus and a photograph of a mounted crystal are shown in Fig. 2(b). The resistivity ρ_{xx} is measured in the same direction as the applied pressure. Simultaneous measurement of magnetic susceptibility was performed using a detachable drive and pickup coil placed directly above the sample. We rely exclusively on susceptibility measurements to determine T_c , to avoid being deceived by percolating higher- T_c current paths. Measurements were done with standard ac methods, at drive frequencies of 50–500 Hz and

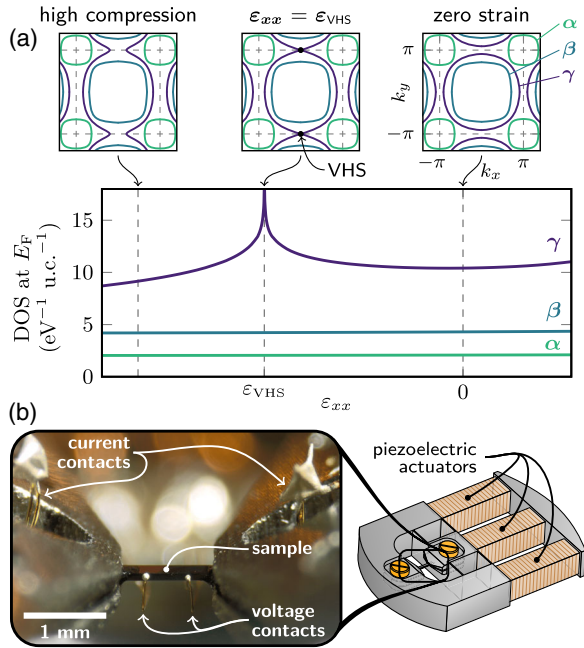


FIG. 2. (a) Sr_2RuO_4 Fermi surface and density of states at the Fermi level as a function of applied anisotropic strain, calculated using a tight-binding model derived from the experimentally determined Fermi surface at ambient pressure [31] and introducing the simplest strain dependence for the hopping terms. See [20] for further simulation details. Fermi surfaces at three representative compressions highlight the Lifshitz transition of the γ surface. (b) A sample mounted for resistivity measurements under uniaxial pressure and a schematic of the piezoelectric-based device that generates the pressure.

0.1–10 kHz, respectively, for resistivity and susceptibility. Uniaxial pressure was applied using the piezoelectric actuators illustrated in Fig. 2(b), as described in more detail in Refs. [23,24,30,33,34]. After some slipping of the sample mounting epoxy during initial compression, all resistivity data repeated through multiple strain cycles, indicating that the sample remained within its elastic limit. Two samples were studied to ensure reproducibility; further details are given in [20].

In Fig. 3, we show $\rho_{xx}(T)$ at various applied compressions. Consistent with the high T_c of 1.5 K at zero strain, the residual resistivity ρ_{res} is less than 100 n Ω cm, corresponding to an impurity mean free path in excess of 1 μm [35]. The resistivity of the unstrained sample follows a quadratic form, $\rho = \rho_{\text{res}} + AT^2$, up to ~ 20 K [see Fig. 3(a)], as has been firmly demonstrated in previous studies [36,37]. At lower pressures, the resistivity increases across a broad temperature range [Fig. 3(b)]. At $\epsilon_{xx} \sim -0.5\%$ the resistivity at low

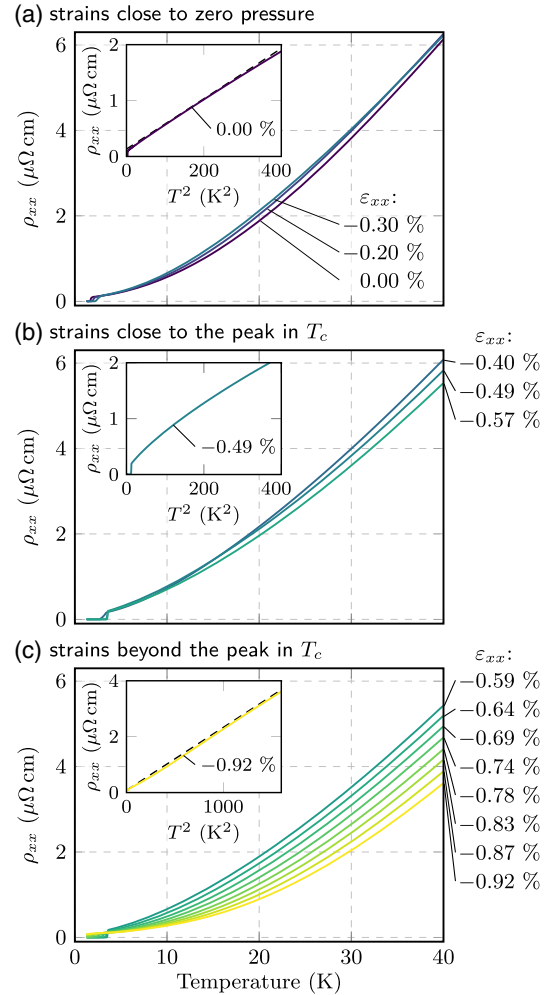


FIG. 3. Temperature dependence of the resistivity ρ_{xx} at a variety of $[100]$ compressive strains: (a) low strains, (b) strains close to the peak in T_c , and (c) strains well beyond the peak in T_c . The insets show that at low temperatures $\rho_{xx}(T)$ is quadratic at low and high strains, but not near the peak in T_c .

temperatures reaches a maximum, and $\rho(T)$ deviates strongly from a quadratic temperature dependence, as shown both in the main plot of Fig. 3(b) and in the inset. With further compression, the resistivity rapidly decreases and a quadratic temperature dependence is restored. By $\epsilon_{xx} = -0.92\%$, the resistivity is almost perfectly quadratic to over 30 K, with the coefficient A reduced to $\sim 40\%$ of its value in the unstrained material [Fig. 3(c)].

We illustrate the strain-dependent evolution of the resistivity in more detail in Fig. 4, and also show a more precise comparison with the evolution of the superconductivity. In Fig. 4(a), we show a logarithmic derivative plot that gives an indication of the strain-dependent power δ associated with a postulated $\rho = \rho_{\text{res}} + BT^\delta$ temperature dependence. ρ_{res} was allowed to vary with strain; however, it is so small that fixing it at a constant value instead barely changes the resulting plot [20]. δ is found to drop from two at low and high strains to ~ 1.5 at $\epsilon_{xx} = -0.5\%$. In Fig. 4(b), we show the quadratic coefficient A versus strain, for strains at which a low-temperature quadratic dependence was resolvable. A increases as ϵ_{xx} approaches -0.5% , then decreases dramatically on the other side. In Fig. 4(c), we plot the results of a measurement of the resistivity measured under continuous strain tuning at 4.5 K (chosen to be 1 K higher than the maximum T_c , to be free of any influence of superconductivity). This plot makes clear that at low temperatures ρ_{xx} peaks at the same strain, $\epsilon_{xx} \approx -0.5\%$, where δ is a minimum. Finally, in Fig. 4(d), we plot T_c and $\rho_{xx}(T = 4.5\text{K})$ against ϵ_{xx} both for this sample and for a second sample with a slightly lower residual resistivity. The magnitude of the resistivity increase is approximately the same for both samples and for both the resistivity peaks at a slightly lower compression than T_c .

As noted above, one mechanism by which the peak in T_c might not correspond to the van Hove singularity is if superconductivity is cut off by a different order promoted by proximity to the VHS. This is the prediction of the functional renormalization group calculations on uniaxially pressurized Sr_2RuO_4 of Ref. [32], which predict formation of spin density wave order. However, there is no indication of any ordering transition in any of the $\rho_{xx}(T)$ curves, either before or after the peak in T_c . Also, $\rho_{xx}(T)$ falls on the other side of the peak, whereas, especially at low temperatures, opening of a magnetic gap should generally cause resistivity to increase.

Taken together, we believe that the data shown in Figs. 3 and 4 give strong evidence that we have successfully traversed the VHS in Sr_2RuO_4 . This VHS has previously been reached in a biaxial way, with the γ sheet connecting along both the k_x and k_y directions, through chemical substitution of La^{3+} onto the Sr site [38,39], and epitaxial growth of Sr_2RuO_4 and Ba_2RuO_4 thin films [19]. In both cases, the resistivity exponent δ dropped to ≈ 1.4 , similar to our result. The novelty of our results is the much lower level of disorder. In these studies, the residual resistivity at the

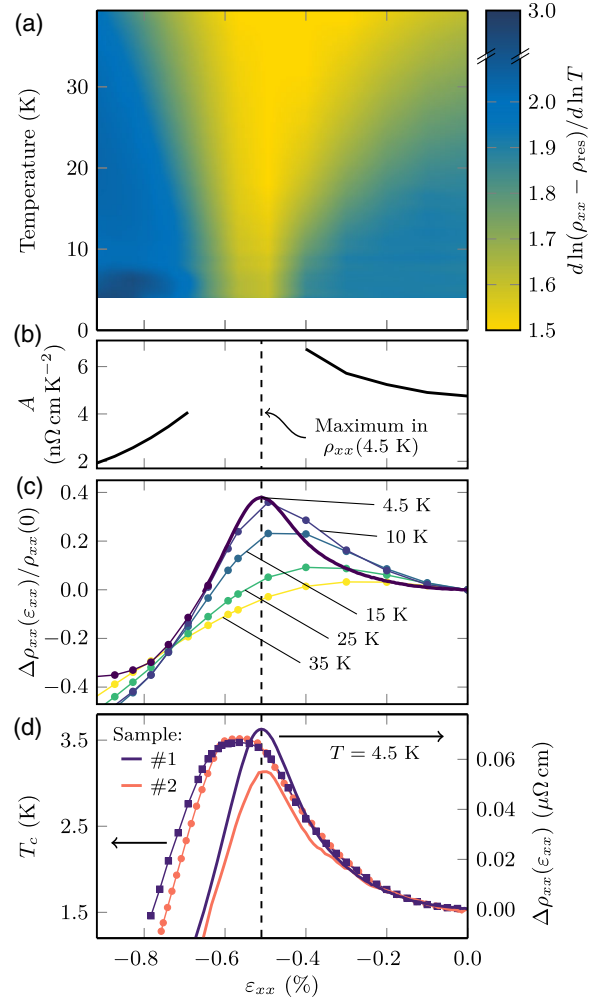


FIG. 4. (a) Resistivity temperature exponent δ plotted against temperature and strain. ρ_{res} was first extracted from fits of the type $\rho = \rho_{\text{res}} + BT^\delta$, then δ was calculated as a function of temperature by $d \ln(\rho - \rho_{\text{res}})/d \ln T$ [20]. (b) A , of $\rho_{xx} = \rho_{\text{res}} + AT^2$, at strains where a T^2 fit performs satisfactorily below 10 K. (c) Elasto-resistance at various temperatures. The data at 4.5 K and up to $\epsilon_{xx} \approx -0.7\%$ were recorded in a continuous strain ramp, while all other data are interpolations of the data in Fig. 3. (d) Comparison of the strain dependence of T_c , measured by magnetic susceptibility, and the resistivity enhancement under continuous strain tuning at 4.5 K. For sample 1, the sample whose data are shown in panels (a)–(c), $\rho_{\text{res}} = 80 \text{ n}\Omega \text{ cm}$ and $\rho_{xx}(\epsilon_{xx} = 0, T = 4.5 \text{ K}) = 190 \text{ n}\Omega \text{ cm}$. For sample 2, these values are 20 and 95 $\text{n}\Omega \text{ cm}$, respectively. For sample 2, T_c was found to peak at a nominal strain of -0.59% , as compared with -0.56% for sample 1. This difference is well within the error, and so to facilitate comparison, we scale the strain scale of sample 2 to match sample 1 at the peak in T_c .

VHS was ~ 50 and ~ 500 times, respectively, as large as in the present study. The inelastic component of the resistivity exceeded the residual resistivity only above ~ 35 and 125 K , respectively, raising concern about the effect of disorder on power laws extracted at much lower temperatures. We believe that the much lower level of disorder

here, the fact that the data in Figs. 3 and 4 cover a full decade of temperature above the maximum T_c , and that the Fermi surface of Sr_2RuO_4 is well known means that our results can set an experimental benchmark for testing theories of transport across Lifshitz transitions. We close with a discussion of what is known so far and the extent to which it applies to our results.

The effect on resistivity of traversing a van Hove singularity has been studied in idealized single-band models, taking into account the energy dependence of the density of states, electron-electron umklapp processes, and impurity scattering. Depending on the form postulated for the density of states, variational calculations using Boltzmann transport theory in the relaxation time approximation have discussed resistivities of the form $\rho(T) = \rho_{\text{res}} + bT^2 \ln(c/T)$ or $\rho(T) = \rho_{\text{res}} + bT^{3/2}$ [9]. Within experimental uncertainties, these two possibilities cannot be distinguished; see Fig. 5. The fits extrapolate very differently below T_c , however, so it will be valuable to attempt to extract the normal-state resistivity below T_c by suppressing the superconductivity with a field. At the VHS, a field of 1.5 T is required [30], and the strong magneto-resistivity of Sr_2RuO_4 [37] makes this a nontrivial task.

Numerical calculations that go beyond the relaxation time approximation have been performed [40,41], and these also predict $\delta < 2$ at Lifshitz transitions. The amount by which δ is reduced depends on the degree of nesting of the Fermi surface; $\delta = 1$ is predicted for perfect nesting.

The evolution of the quadratic coefficient A may allow precision testing of theories of dissipation due to electron-electron scattering. The Kadowaki-Woods ratio A/γ^2 , where γ is the Sommerfeld coefficient, varies widely between

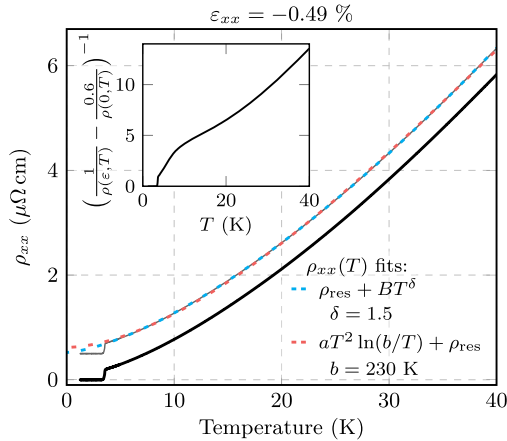


FIG. 5. A comparison of different fitting functions for the temperature dependence of the resistivity at $\epsilon_{xx} = -0.49\%$. The data are plotted alone, and then together with the fits and offset by $0.5 \mu\Omega \text{ cm}$. Both fits are made over the range 4–40 K. The inset shows the same resistivity curve after subtracting 60% of the zero strain conductivity, estimated to be the contribution of the γ band if the scattering rate of the α and β sheet carriers is unaffected by the traversal of the Lifshitz point on the γ sheet.

material classes, but is predicted to hold constant when the strength of electronic correlations varies on a given bare (i.e., nonrenormalized) band structure [42–45]. Hydrostatic pressure on Sr_2RuO_4 causes a decrease in both T_c and A , suggesting a reduction in electronic correlation [46]. The dependence of A on uniaxial pressure is surprisingly strong. In our tight-binding model of Fig. 2, where band renormalizations are held constant as strain is varied, the density of states barely changes up to $\sim 80\%$ of the way to the VHS. Density functional theory (DFT) calculations indicate only a $\sim 5\%$ increase in DOS over this range [30]. However, A increases by $\sim 40\%$. Likewise, at $\epsilon_{xx} \sim -0.9\%$, well beyond the VHS, the tight-binding model and DFT calculations indicate a drop in the DOS of $\sim 20\%$ and $\sim 10\%$, respectively, while A falls by 60%. In other words, the dependence of A on the nonrenormalized DOS is stronger than quadratic, and we see two possible explanations. (1) Electronic interactions become stronger near the VHS, and the Kadowaki-Woods ratio is expected to remain unchanged. (2) The changes in A are driven mainly by the changes in Fermi surface shape of the type probed in Refs. [40,41], and the Kadowaki-Woods ratio is not expected to be constant.

Finally, we note that, although the model temperature dependences fit the data well, they were derived for single-band metals, and it is questionable whether they should even apply to Sr_2RuO_4 . As illustrated in Fig. 2(a), in Sr_2RuO_4 , the Lifshitz transition occurs on the γ Fermi surface sheet alone. At zero strain, the average Fermi velocities of each sheet are known, and so for a sheet-independent scattering rate, it is straightforward to estimate that the α and β sheets contribute over 60% of the conductivity. Under the postulate that the scattering rate of the α and β sheet carriers is unaffected by the traversal of the Lifshitz point on the γ sheet, the implied contribution of the γ sheet to the resistivity at -0.49% strain is shown in the inset to Fig. 5. It is qualitatively different from any single-band prediction. The likely implication is that the scattering rates on the α and β sheets are affected in a similar way to that on the γ sheet. However, it seems far from obvious that this should automatically be the case, and it would be interesting to see full multiband calculations for Sr_2RuO_4 to assess the extent to which it can be understood using conventional theories of metallic transport.

In conclusion, we believe that the results that we have presented in this Letter represent an experimental benchmark for the effects on resistivity of undergoing a Lifshitz transition against a background of very weak disorder. Our results stimulate further theoretical work on this topic and highlight the suitability of uniaxial stress for probing this class of physics.

The raw data for this publication may be downloaded at [47].

We thank J. Schmalian, E. Berg, and M. Sigrist for useful discussions and H. Takatsu for sample growth. We

acknowledge the support of the Max Planck Society and the UK Engineering and Physical Sciences Research Council under Grants No. EP/I031014/1 and No. EP/G03673X/1. Y. M. acknowledges the support by the Japan Society for the Promotion of Science Grants-in-Aid for Scientific Research (KAKENHI) JP15H05852 and JP15K21717.

*barber@cpfs.mpg.de

†Present address: ISIS Facility, Rutherford Appleton Laboratory, Chilton, Didcot OX11 0QX, United Kingdom.

‡andy.mackenzie@cpfs.mpg.de

§hicks@cpfs.mpg.de

- [1] I. M. Lifshitz, Anomalies of electron characteristics of a metal in the high pressure region, *Zh. Eksp. Teor. Fiz.* **38**, 1569 (1960) [*Sov. Phys. JETP* **11**, 1130 (1960)].
- [2] G. E. Volovik, Topological Lifshitz transitions, *Low Temp. Phys.* **43**, 47 (2017).
- [3] C. C. Tsuei, D. M. Newns, C. C. Chi, and P. C. Pattnaik, Anomalous isotope effect and van Hove singularity in superconducting Cu oxides, *Phys. Rev. Lett.* **65**, 2724 (1990).
- [4] R. S. Markiewicz, A survey of the van Hove scenario for high- T_c superconductivity with special emphasis on pseudogaps and striped phases, *J. Phys. Chem. Solids* **58**, 1179 (1997).
- [5] C. Liu, T. Kondo, R. M. Fernandes, A. D. Palczewski, E. D. Mun, N. Ni, A. N. Thaler, A. Bostwick, E. Rotenberg, J. Schmalian, S. L. Bud'ko, P. C. Canfield, and A. Kaminski, Evidence for a Lifshitz transition in electron-doped iron arsenic superconductors at the onset of superconductivity, *Nat. Phys.* **6**, 419 (2010).
- [6] Y. Quan and W. E. Pickett, Van Hove singularities and spectral smearing in high-temperature superconducting H_3S , *Phys. Rev. B* **93**, 104526 (2016).
- [7] J. L. Sarrao and J. D. Thompson, Superconductivity in cerium- and plutonium-based '115' materials, *J. Phys. Soc. Jpn.* **76**, 051013 (2007).
- [8] E. E. Rodriguez, D. A. Sokolov, C. Stock, M. A. Green, O. Sobolev, J. A. Rodriguez-Rivera, H. Cao, and A. Daoud-Aladine, Magnetic and structural properties near the Lifshitz point in $Fe_{1+x}Te$, *Phys. Rev. B* **88**, 165110 (2013).
- [9] R. Hlubina, Effect of impurities on the transport properties in the van Hove scenario, *Phys. Rev. B* **53**, 11344 (1996).
- [10] A. A. Varlamov, V. S. Egorov, and A. Pantsulaya, Kinetic properties of metals near electronic topological transitions (2 1/2-order transitions), *Adv. Phys.* **38**, 469 (1989).
- [11] E. A. Yelland, J. M. Barraclough, W. Wang, K. V. Kamenev, and A. D. Huxley, High-field superconductivity at an electronic topological transition in URhGe, *Nat. Phys.* **7**, 890 (2011).
- [12] H. Pfau, R. Daou, S. Lausberg, H. R. Naren, M. Brando, S. Friedemann, S. Wirth, T. Westerkamp, U. Stockert, P. Gegenwart, C. Krellner, C. Geibel, G. Zwirgagl, and F. Steglich, Interplay between Kondo Suppression and Lifshitz Transitions in $YbRh_2Si_2$ at High Magnetic Fields, *Phys. Rev. Lett.* **110**, 256403 (2013).
- [13] D. Aoki, G. Seyfarth, A. Pourret, A. Gourgout, A. McCollam, J. A. N. Bruin, Y. Krupko, and I. Sheikin, Field-Induced Lifshitz Transition without Metamagnetism in $CeIrIn_5$, *Phys. Rev. Lett.* **116**, 037202 (2016).
- [14] G. Bastien, A. Gourgout, D. Aoki, A. Pourret, I. Sheikin, G. Seyfarth, J. Flouquet, and G. Knebel, Lifshitz Transitions in the Ferromagnetic Superconductor UCoGe, *Phys. Rev. Lett.* **117**, 206401 (2016).
- [15] D. S. Grachtrup, N. Steinki, S. Stillo, Z. Cakir, G. Zwirgagl, Y. Krupko, I. Sheikin, M. Jaime, and J. A. Mydosh, Magnetic phase diagram and electronic structure of UPt_2Si_2 at high magnetic fields: A possible field-induced Lifshitz transition, *Phys. Rev. B* **95**, 134422 (2017).
- [16] H. Pfau, R. Daou, S. Friedemann, S. Karbassi, S. Ghannadzadeh, R. Kuchler, S. Hamann, A. Steppke, D. Sun, M. König, A. P. Mackenzie, K. Kliemt, C. Krellner, and M. Brando, Cascade of Magnetic-Field-Induced Lifshitz Transitions in the Ferromagnetic Kondo Lattice Material $YbNi_4P_2$, *Phys. Rev. Lett.* **119**, 126402 (2017).
- [17] C. W. Chu, T. F. Smith, and W. E. Gardner, Study of Fermi-surface topology changes in rhenium and dilute Re solid solutions from T_c measurements at high pressure, *Phys. Rev. B* **1**, 214 (1970).
- [18] D. R. Overcash, T. Davis, J. W. Cook, and M. J. Skove, Stress-Induced Electronic Transition (2.5 Order) in Al, *Phys. Rev. Lett.* **46**, 287 (1981).
- [19] B. Burganov, C. Adamo, A. Mulder, M. Uchida, P. D. C. King, J. W. Harter, D. E. Shai, A. S. Gibbs, A. P. Mackenzie, R. Uecker, M. Bruetzmann, M. R. Beasley, C. J. Fennie, D. G. Schlom, and K. M. Shen, Strain Control of Fermiology and Many-Body Interactions in Two-Dimensional Ruthenates, *Phys. Rev. Lett.* **116**, 197003 (2016).
- [20] See Supplemental Material at <http://link.aps.org/supplemental/10.1103/PhysRevLett.120.076602> for additional experimental data, further details of the experimental technique, and a description of the tight-binding simulations, which includes Ref. [21].
- [21] J. Paglione, C. Lupien, W. A. MacFarlane, J. M. Perz, L. Taillefer, Z. Q. Mao, and Y. Maeno, Elastic tensor of Sr_2RuO_4 , *Phys. Rev. B* **65**, 220506 (2002).
- [22] C. L. Watlington, J. W. Cook, and M. J. Skove, Effect of large uniaxial stress on the superconducting transition temperature of zinc and cadmium, *Phys. Rev. B* **15**, 1370 (1977).
- [23] C. W. Hicks, M. E. Barber, S. D. Edkins, D. O. Brodsky, and A. P. Mackenzie, Piezoelectric-based apparatus for strain tuning, *Rev. Sci. Instrum.* **85**, 065003 (2014).
- [24] C. W. Hicks, D. O. Brodsky, E. A. Yelland, A. S. Gibbs, J. A. N. Bruin, M. E. Barber, S. D. Edkins, K. Nishimura, S. Yonezawa, Y. Maeno, and A. P. Mackenzie, Strong increase of T_c of Sr_2RuO_4 under both tensile and compressive strain, *Science* **344**, 283 (2014).
- [25] Y. Maeno, H. Hashimoto, K. Yoshida, S. Nishizaki, T. Fujita, J. G. Bednorz, and F. Lichtenberg, Superconductivity in a layered perovskite without copper, *Nature (London)* **372**, 532 (1994).
- [26] A. P. Mackenzie and Y. Maeno, The superconductivity of Sr_2RuO_4 and the physics of spin-triplet pairing, *Rev. Mod. Phys.* **75**, 657 (2003).
- [27] Y. Maeno, S. Kittaka, T. Nomura, S. Yonezawa, and K. Ishida, Evaluation of Spin-Triplet Superconductivity in Sr_2RuO_4 , *J. Phys. Soc. Jpn.* **81**, 011009 (2012).

- [28] C. Kallin, Chiral p-wave order in Sr_2RuO_4 , *Rep. Prog. Phys.* **75**, 042501 (2012).
- [29] A. P. Mackenzie, T. Scaffidi, C. W. Hicks, and Y. Maeno, Even odder after twenty-three years: the superconducting order parameter puzzle of Sr_2RuO_4 , *npj Quantum Mater.* **2**, 40 (2017).
- [30] A. Steppke, L. Zhao, M. E. Barber, T. Scaffidi, F. Jerzembeck, H. Rosner, A. S. Gibbs, Y. Maeno, S. H. Simon, A. P. Mackenzie, and C. W. Hicks, Strong peak in T_c of Sr_2RuO_4 under uniaxial pressure, *Science* **355**, eaaf9398 (2017).
- [31] C. Bergemann, A. P. Mackenzie, S. R. Julian, D. Forsythe, and E. Ohmichi, Quasi-two-dimensional Fermi liquid properties of the unconventional superconductor Sr_2RuO_4 , *Adv. Phys.* **52**, 639 (2003).
- [32] Y.-C. Liu, F.-C. Zhang, T. M. Rice, and Q.-H. Wang, Theory of the evolution of superconductivity in Sr_2RuO_4 under anisotropic strain, *npj Quantum Mater.* **2**, 12 (2017).
- [33] D. O. Brodsky, M. E. Barber, J. A. N. Bruin, R. A. Borzi, S. A. Grigera, R. S. Perry, A. P. Mackenzie, and C. W. Hicks, Strain and vector magnetic field tuning of the anomalous phase in $\text{Sr}_3\text{Ru}_2\text{O}_7$, *Sci. Adv.* **3**, e1501804 (2017).
- [34] M. E. Barber, Ph.D. thesis, University of St. Andrews, 2017.
- [35] A. P. Mackenzie, R. K. W. Haselwimmer, A. W. Tyler, G. G. Lonzarich, Y. Mori, S. Nishizaki, and Y. Maeno, Extremely Strong Dependence of Superconductivity on Disorder in Sr_2RuO_4 , *Phys. Rev. Lett.* **80**, 161 (1998).
- [36] Y. Maeno, K. Yoshida, H. Hashimoto, S. Nishizaki, S.-I. Ikeda, M. Nohara, T. Fujita, A. P. Mackenzie, N. E. Hussey, J. G. Bednorz, and F. Lichtenberg, Two-dimensional Fermi liquid behavior of the superconductor Sr_2RuO_4 , *J. Phys. Soc. Jpn.* **66**, 1405 (1997).
- [37] N. E. Hussey, A. P. Mackenzie, J. R. Cooper, Y. Maeno, S. Nishizaki, and T. Fujita, Normal-state magnetoresistance of Sr_2RuO_4 , *Phys. Rev. B* **57**, 5505 (1998).
- [38] N. Kikugawa, C. Bergemann, A. P. Mackenzie, and Y. Maeno, Band-selective modification of the magnetic fluctuations in Sr_2RuO_4 : A study of substitution effects, *Phys. Rev. B* **70**, 134520 (2004).
- [39] K. M. Shen, N. Kikugawa, C. Bergemann, L. Balicas, F. Baumberger, W. Meevasana, N. J. C. Ingle, Y. Maeno, Z.-X. Shen, and A. P. Mackenzie, Evolution of the Fermi Surface and Quasiparticle Renormalization through a van Hove Singularity in $\text{Sr}_{2-y}\text{La}_y\text{RuO}_4$, *Phys. Rev. Lett.* **99**, 187001 (2007).
- [40] J. M. Buhmann, Unconventional scaling of resistivity in two-dimensional Fermi liquids, *Phys. Rev. B* **88**, 245128 (2013).
- [41] J. M. Buhmann, Ph.D. thesis, ETH Zurich, 2013.
- [42] M. J. Rice, Electron-Electron Scattering in Transition Metals, *Phys. Rev. Lett.* **20**, 1439 (1968).
- [43] K. Kadowaki and S. Woods, Universal relationship of the resistivity and specific heat in heavy-Fermion compounds, *Solid State Commun.* **58**, 507 (1986).
- [44] N. E. Hussey, Non-generality of the Kadowaki-Woods Ratio in Correlated Oxides, *J. Phys. Soc. Jpn.* **74**, 1107 (2005).
- [45] A. C. Jacko, J. O. Fjærestad, and B. J. Powell, A unified explanation of the Kadowaki-Woods ratio in strongly correlated metals, *Nat. Phys.* **5**, 422 (2009).
- [46] D. Forsythe, S. R. Julian, C. Bergemann, E. Pugh, M. J. Steiner, P. L. Alireza, G. J. McMullan, F. Nakamura, R. K. W. Haselwimmer, I. R. Walker, S. S. Saxena, G. G. Lonzarich, A. P. Mackenzie, Z. Q. Mao, and Y. Maeno, Evolution of Fermi-Liquid Interactions in Sr_2RuO_4 under Pressure, *Phys. Rev. Lett.* **89**, 166402 (2002).
- [47] <http://dx.doi.org/10.17617/3.16>.